Analysis of human chorionic gonadotropin-monoclonal antibody interaction in BIAcore

BANERJEE ASHISH and GUNDLUPET SATYANARAYANA MURTHY*

Department of Molecular Reproduction, Development and Genetics, Indian Institute of Science, Bangalore 560 012, India

**Corresponding author (Fax, 91-80-23600999; Email, crbsat@mrdg.iisc.ernet.in)*

Kinetic studies of macromolecular ligand-ligate interaction have generated ample interest since the advent of plasmon resonance based instruments like BIAcore. Most of the studies reported in literature assume a simple 1 : 1 Langmuir binding and complete reversibility of the system. However we observed that in a high affinity antigen-antibody system [human chorionic gonadotropin-monoclonal antibody (hCG-mAb)] dissociation is insignificant and the sensogram data cannot be used to measure the equilibrium and kinetic parameters. At low concentrations of mAb the complete sensogram could be fitted to a single exponential. Interestingly we found that at higher mAb concentrations, the binding data did not conform to a simple bimolecular model. Instead, the data fitted a two-step model, which may be because of surface heterogeneity of affinity sites. In this paper, we report on the global fit of the sensograms. We have developed a method by which a single two-minute sensogram can be used in high affinity systems to measure the association rate constant of the reaction and the functional capacity of the ligand (hCG) immobilized on the chip. We provide a rational explanation for the discrepancies generally observed in most of the BIAcore sensograms.

[Ashish B and Murthy G S 2004 Analysis of human chorionic gonadotropin-monoclonal antibody interaction in BIAcore; *J. Biosci*. **29** 57–66]

1. Introduction

Studies of the kinetics of molecular interactions provide a wealth of information on the mechanism of the same. Such studies involving macromolecules extensively employ BIAcore (surface plasmon resonance-based equipment). Analysis of the binding profiles carried out by conventional kinetics approaches assume that the reaction between the ligand and ligate is freely reversible (Chaiken *et al* 1992; Malmqvist 1993; Pellequer and Van Regenmortel 1993). However, in several instances, especially in those involving macromolecular reactants of high affinity the dissociation is unsatisfactory (Nieba *et al* 1996; McCloskey *et al* 1997; Bornhauser 1998) and frequently overlooked in the analysis (Muslin *et al* 1996; McCloskey *et al* 1997; Yamaji *et al* 1998). The only parameter that can be obtained from such bindings is the association rate constant (k_{+1}). Our attempt at dissociating the human chorionic gonadotropin-monoclonal antibody (hCG-mAb) complex resulted in less than 5% dissociation in the BIAcore even with several hours of washing. Though a survey of literature shows that the dissociation profiles are not ideal (Muslin *et al* 1996; Yamaji *et al* 1998), this observation has largely been neglected during analysis, and rarely global fits of the sensograms are provided, though the affinity constants are presented in communications. One possible reason we could ascribe for the failure of the software to provide a satisfactory global fit of the sensogram is that the assumption of complete reversibility may be in error. In this paper we report the analysis of the interaction of hCG with several mAbs in BIAcore and obtain a global fit of the association on the assumption that the reaction is apparently nonreversible. Incidentally we also show that the association rate constant of the interaction and the capacity of the immobilized ligand can be obtained from a single two-minute sensogram. Our

Keywords. Antigen; association rate constant; BIAcore; high affinity; monoclonal antibody; non-dissociable

analysis may hold good for several other apparently non-dissociable systems in BIAcore.

2. Materials and methods

2.1 *Reagents*

hCG was locally prepared by the standard procedure using immuno-affinity chromatography (Murthy and Moudgal 1986; Venkatesh *et al* 1995; Venkatesh and Murthy 1997). mAbs were local preparations with specificities for α-subunit (VM15, VM10 and C10) and $\alpha\beta$-heterodimer (VM11). All the mAbs belonged to the IgG1 class.

2.2 *Capacity determination of mAbs*

The principle of the method is based on the theory of equivalence point in antigen-antibody interaction and is explained in detail earlier (Banerjee *et al* 2002). In brief when a known quantity of antigen is incubated with different quantities of the antibody, the presence of free antigen or antibody will be minimum at the equivalence point. Binding of IhCG to immobilized mAb will be affected by such mixtures, and binding is least affected at the point of equivalence. Experimentally 100 ng of hCG in RIA buffer (0·1% BSA in 50 mM phosphate buffered saline) was incubated overnight with varying volumes (10 µl–200 µl) of known mAb dilution in a total volume of 300 µl and 20 µl of the incubation mixture was added to mAb-coated microtiter wells (Banerjee *et al* 2002) along with 50 µl of ^{125}IhCG (radio-iodinated hCG, 50,000 cpm). Binding was carried out for 2 h and the radioactivity bound was measured in a multigamma counter.

2.3 *Immobilization of hCG on CM5 chip (research grade) and its binding to mAb*

hCG was immobilized on a CM5 chip using the standard procedure for amine coupling. A total immobilization of 226 RUs was achieved. Binding was carried out at constant flow rates of 100 or 50 µl/min of the mAb at various dilutions in hepes buffered saline (BIA certified) in a BIAcore 2000. Dissociations were carried out by passing buffer and/or hCG in buffer. Regeneration of the surface was carried out by injecting 10 mM NaOH for 1 min at a flow rate of 10 µl/min. No loss of binding capacity was observed under these conditions. Thus the same surface was used for all experiments.

2.4 *Global fit of the binding data or the sensogram*

The reaction mechanism used to analyse the global fit is as follows, based on the reaction mechanism proposed for the study of kinetics earlier (Banerjee *et al* 2002), using ^{125}IhCG and immobilized mAb

$$\text{hCG} + \text{mAb} \xrightarrow{k_{+1}} A \xrightarrow{k_{+2}} B, \quad (1)$$

where, '*A*' and '*B*' are two forms of the complex, with *A* having a role in the formation of complex *B*.

2.4a *Rationale for the determination of the rate constant k_{+1}:* The quantum of binding of the mAb to immobilized hCG depends on the concentration of the hCG bound to the chip, dilution of the mAb, and the flow rate of the mAb through the chip. By holding the concentration of mAb at a given level and by ensuring a high flow rate it is possible to keep the rate of binding to < 5% in the sensogram. Under these conditions, the concentration of mAb is considered to be constant and the binding is described by the equation,

$$dx/dt = k_{+1}(C_{\text{hCG}})\,(C_{\text{mAb}}), \quad (2)$$

where dx/dt is the rate of increase of response (experimental data), k_{+1} is the rate constant of association (unknown), C_{hCG} is the effective concentration of hCG on the chip (unknown) and C_{mAb} is the concentration of mAb solution passing through the flow cell (known). C_{hCG} in the above equation can be determined as follows. In a non-reversible system of interaction and at constant C_{mAb} (as < 5% of mAb is adsorbed during the passage of the mAb solution), the saturation by mAb should conform to a perfect single exponential pattern governed by the equation,

$$Y = Y_{\text{max}}\,(1 - e^{-Qt}), \quad (3)$$

where '*Y*' is the amount of mAb bound at time '*t*' (RU_t or response at time '*t*'), Y_{max} is the concentration of hCG on the chip (C_{hCG} or RU_{max}) and *Q* is the pseudo first order rate constant ($k_{+1} \times C_{\text{mAb}}$). Under conditions of partial reversibility, the contribution of the reverse reaction would be insignificant in the early phase of association and so the calculation given above would still hold good. Experimental data consisting of several points can be fitted to the above equation for a single set of C_{hCG} and *Q* values. The best fit in our case was obtained by independently varying C_{hCG} (from 0·1 to 100% of the theoretical value at steps of 0·1%–100% was considered to be 20 times the RU increase observed in 2 min) and *Q* (also varied independently) to obtain theoretical plots. The plot that gave minimum deviation from the experimental points was considered for obtaining the values of Y_{max} and *Q*. The rate constant k_{+1} was calculated using the equation

$$k_{+1} = Q/C_{\text{mAb}}. \quad (4)$$

In an alternate approach the values of RU against time

from the initial portion of the sensogram were analysed by a single phase exponential equation using graph pad prism and the error at each point of time was calculated to obtain average error per point to choose the best fit. This exercise gives the value of k_{+1} and Y_{max} (table 1).

2.4b *Determination of the second rate constant* (k_{+2}) *from the sensogram*: The second step binding of the ligand was obtained in a quantitative fashion by subtracting the contribution of the first phase of the reaction (using Y_{max} and k_{+1} values obtained) from the experimental value at each point of time. The difference contributed for the second step of the binding of the ligand. The graph of bound vs time was plotted on a graph sheet and the intersection on the x-axis was obtained by extrapolation of the graph to find the zero point of the second reaction. (This was possible because of the difference in the rate constants between the first and the second step reactions.) Analysis of the 2nd step of the reaction was then carried out using different mechanisms of the reaction.

2.5 *Analysis of the binding data from literature*

Data from Kalinin *et al* (1995, figure 1a) were converted to percent binding using the following equation and analysed for the two-step fit using the graph pad prism software.

$$\{1 - e^{[1n(1 - R_T/R_E)]}\} \times 100. \quad (5)$$

Data from Thomas *et al* (1999, figure 1B) and Thomas and Surolia (2000, figure 2) were analysed for the two-step fit using the graph pad prism software.

2.5a *Determination of rate constant of binding of IhCG to immobilized mAb on nitrocellulose disc*: mAb adsorbed nitrocellulose disc was taken in 2 ml of the required buffer containing 1–2 lakh cpm/ml at room temperature, and binding of the label was monitored with time by taking the disc out of the reaction solution and counting the radioactivity bound at 3 min interval for 18 min. The binding was found to be linear. k_{+1} is calculated by the equation;

$$k_{+1} = \{(\text{slope})/(^{125}\text{IhCG})\,(\text{mAb})\},$$

where *dx/dt* is the slope of binding, the denominators being the initial concentrations of the ^{125}IhCG and mAb respectively, which were very high compared to the slope of binding.

3. Results and discussion

The concentrations of the mAbs used were determined by measuring the binding ability of the mAbs to hCG. Figure 1 shows the specific binding of IhCG to mAb (VM10) immobilized on microtiter wells in the presence of preincubated mixtures of hCG (100 ng) and the same mAb at different concentrations. At the equivalence point (peak of binding) 50 µl of mAb at 1/8000 dilution neutralizes 100 ng of hCG. Thus the hCG binding capacity of the mAb was calculated to be 16 mg/ml for this mAb ascites. The capacity of other mAbs were determined similarly were VM15 (5 mg/ml) and VM11 (8 mg/ml).

The interaction between hCG and mAb shows very poor reversibility. Figure 2 shows the binding and dissociation of mAb VM15 in HEPES buffer saline (HBS). The dissociation did not exceed 5% even after 5 min of continuous buffer flow. In fact flow of buffer for over 1 h in a separate experiment did not result in any significant increase in dissociation (data not shown).

Figure 3 presents the binding of mAb VM15 to immobilized hCG. The first phase of the curve (0–362 s) presents the binding of mAb to hCG, while 363–557 s indicates the extent of dissociation in buffer, which was less than 7 RUs (< 5%). An attempt has been made to dissociate the mAb by including hCG (10 µg/ml) in the running buffer between 558–673 s. Surprisingly instead of dissociation, binding of the hCG occurred, and the increase in the RU (60RU) exactly corresponded to near saturation of the second arm of the bound mAb (220RU). This binding was fast and could be dissociated completely in the running buffer. This dissociation data when analysed by the two step method reported earlier for IhCG mAb system provided quantitative data on the rate constants of the dissociation and the ratio of the two forms of the complex

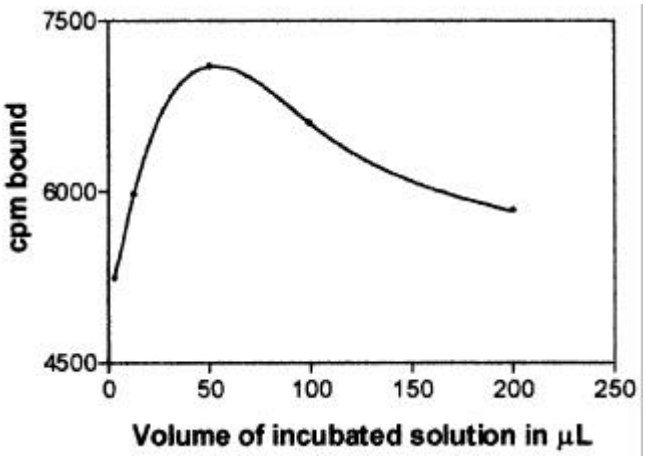

Figure 1. Capacity determination of mAb VM10. For details see §2.

(see figure 3 inset). Additional injection of hCG at 1070 s resulted in a similar increase in the binding of hCG to the hCG-mAb complex, which was also easily dissociable giving similar rate constants ($0{\cdot}11645 \pm 0{\cdot}0108\ s^{-1}$). The dissociation rate constant is several fold higher than that obtained for the same system by the radiolabelled approach (Banerjee *et al* 2002). The reason for this discrepancy is not known at present. During both cycles the mAb did not dissociate as the response obtained in the second injection of hCG was comparable to the first. The reason for the easy dissociation of hCG bound to the other arm remains unknown. Observations indicate that two arms of an mAb are identical and exclusive in their antigen binding. Yet in this case, the hCG bound to the second arm is completely dissociable, while the mAb bound to the solid phase hCG is non-dissociable. This data demonstrate that the mAb does not bind bivalently to surface immobilized hCG and that the binding of mAb to immobilized hCG is apparently nonreversible.

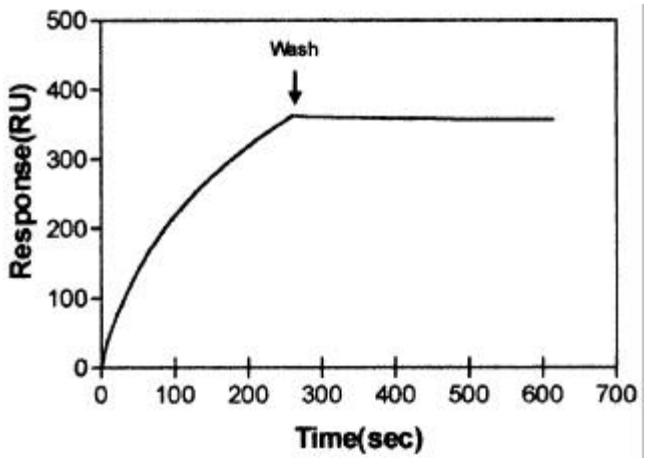

Figure 2. Sensogram showing binding of mAb VM15 (0·0675 μM) to hCG immobilized on CM5 and subsequent washing in HBS.

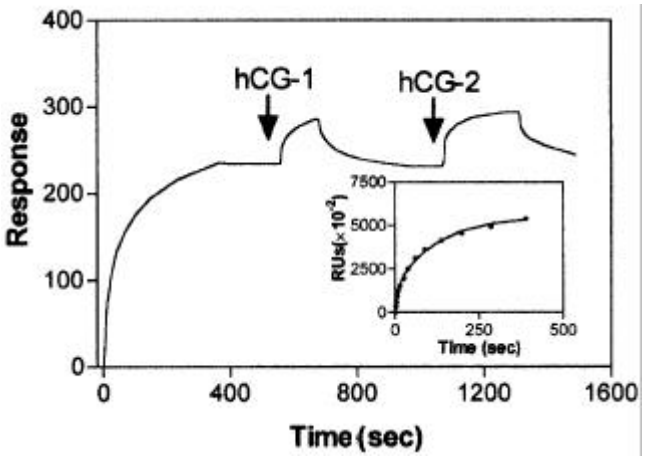

Figure 3. Sensogram showing binding of mAb VM15 (0·0675 μM) to hCG immobilized on CM5 (0–362 s) and subsequent washing in HBS (363–557 s) followed by an injection of hCG (10 μg/ml in HBS) (558–673 s) and flow of buffer until 1069 s followed by another injection of hCG (1070–1274 s) and buffer flow until regeneration of the surface. Flow rate throughout the experiment was 100 μl/min. *Inset*: Analysis of the dissociation during 673–1069 s as per the two-step model (please refer to text and Banerjee *et al* 2002).

Figure 4a presents the binding of mAb VM11 at very low concentration to immobilized hCG. The sensogram was analysed for a nonreversible reaction as described in §2. The complete data of binding (0–300 s) fitted to single step nonreversible reaction kinetics. However, when the mAb concentration was increased (figure 4b, c, d) the sensogram data instead fitted to the two-step model, the first phase (1st step in figure 4) was obtained by analysing the initial part of the binding curve (0–60 s) using equation 3. The second phase of binding (2nd step in figure 4) was obtained by subtracting the 1st step curve from the total binding (Global in figure 4) at each point. Thus at very low concentration of mAb the association could be fitted to a one step exponential model. However as the concentration of the mAb increased (as low as 4–10-fold) the simple mechanism failed to provide a global fit, indicating towards a more complex reaction mechanism. The rate of the second reaction had a linear relationship with the concentration of the mAb. In addition the lag period observed decreased as the concentration of the mAb increased (150 s for 0·108 μM, 75 s for 0·216 μM and only 30 s for 0·432 μM). The second step which identified in the global fit, may be arising out of the heterogeneity of binding sites upon immobilization of hCG on the chip.

Figure 5 presents the global analysis of the binding of VM15 mAb to hCG at two concentration. In this case, the second phase of binding is more striking in this case. As in VM11 (figure 4) the lag phase of the second phase decreased at increased mAb concentrations (figure 5a, b, 2nd step). The 2nd step curves were plotted, and the linear part of the initial phase of binding was extrapolated to the x-axis. Figure 5c, d show the fit of the second phase of the interaction to a pseudo first order reaction model. The Y_{max} and rate constants obtained (2nd step) for two concentrations of mAb are comparable, indicating that these parameters too are concentration independent. Thus the interaction of mAb to immobilized hCG in BIAcore can be explained on the basis of equation 1. That such a behaviour of monoclonal antibodies is not unique to ascites, was ascertained by the use of a hybridoma culture supernatant, C10. Figure 6a, b show analyses of binding of mAb C10 to hCG. As observed for other mAbs, for this mAb as well the lag period is inversely related to the concentration of the mAb, and the second binding fitted to a pseudo first order model. The second phase binding was very specific and did not occur with any other anti-

body. Binding of a monoclonal antibody to hFSH to preformed hCG-mAb was not observed, clearly indicating that the binding observed is indeed specific (data not shown).

Table 1 shows the consolidation of the data obtained with various mAbs binding to the hCG in BIAcore sensograms. The values of Y_{max} and k_{+1} obtained are reproducible with good consistency. The flow rate does not seem to affect these parameters, as they are comparable at flow rates of 50 and 100 µl/min. These data indicate that the concentration of the mAbs used in these experiments is in excess of what is bound. In other words the binding is not mass transport limited. The average Y_{max} is ~ 220 RUs across all the antibodies. Theoretically the Y_{max} should have been ~ 900 RUs taking into account a total immobilization of 226 RUs of hCG (considering that the molecular weight of hCG is 37 kDa and that of IgG is 150 kDa). Thus our data indicates that immobilization renders ~ 75% of the affinity sites partially/completely inaccessible. In other words only ~ 25% of the binding sites are completely exposed for the mAb to bind. Surfaces having higher immobilization densities behaved similarly, indicating that sterical blocking of the binding sites is independent of the extent of immobilization (data not shown). The kinetic constants obtained for the association using radiolabelled hCG and immobilized mAb on the nitrocellulose (figure 7) is also presented in the table. The rate constants obtained are comparable. The differences in k_{+1}'s are marginal considering that the methods are distinctly different.

Analysis of the data for the binding of Con-A to CM-dextran (Kalinin *et al* 1995) is analysed by the method developed for the hCG-mAb system (figure 8). The total binding which is depicted by the legend 'Global' in figure 8, could not be fitted into a single exponential equation. The binding profile could be fitted to the two-step model (equation 1), and the second step binding has a lag period. This data, as reported (Kalinin *et al* 1995) show poor/incomplete dissociation. Binding of a cyclic peptide to lipid-A (Thomas *et al* 1999) has also been re-analysed based on our approach, as significant part of the complex remained undissociated in this case. The analysis of the binding data conforms to the two-step model (figure 9). In contrast another data involving the binding of UEA1 to H-antigenic fucolipid (Thomas and Surolia 2000), which is completely dissociable, fitted into a single exponential equation (inset to figure 9). Thus our own ex-

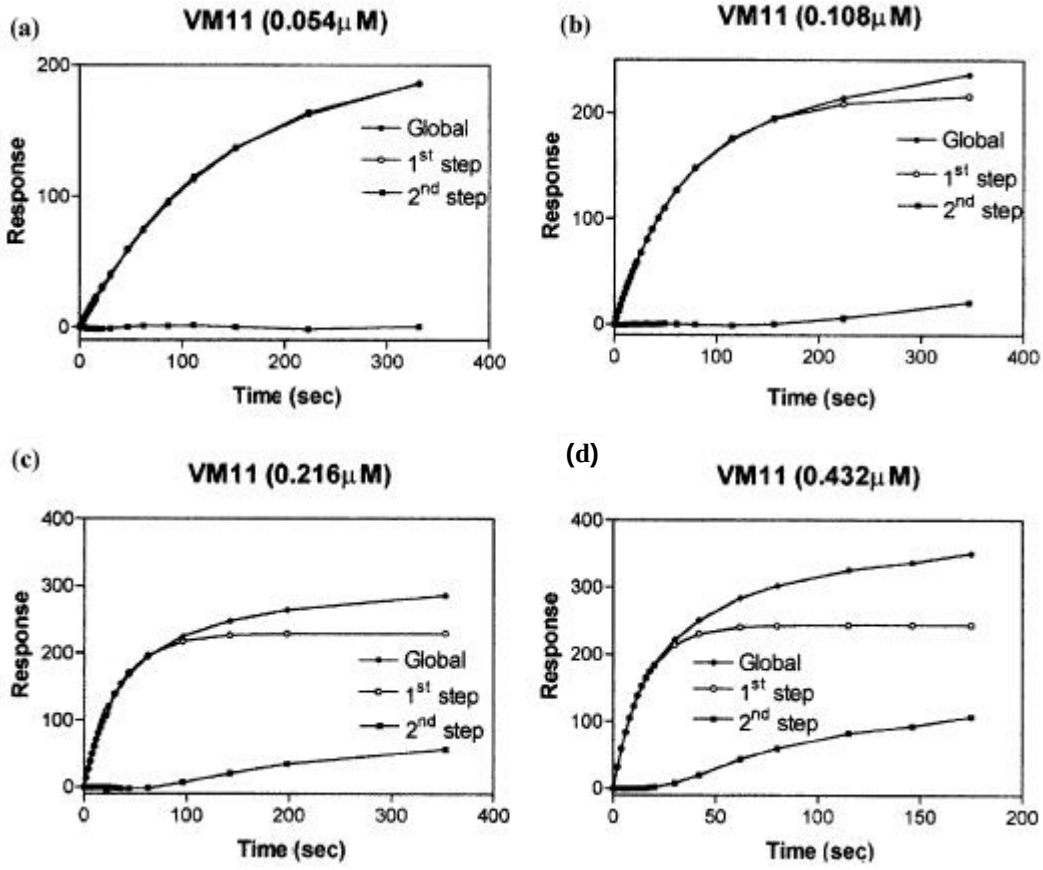

Figure 4. Binding analysis of mAb VM11 at specified concentrations to immobilized hCG.

periments based on four mAbs and two experimental data from literature suggest that for systems showing partial dissociation a simple bimolecular reaction model does not explain the binding profile. The nonconformity to this model may be because of several reasons. In the case of hCG-mAb, the reason probably is due to heterogeneity of the binding sites on the surface. A global fit of the sensogram can be however be obtained, at least for our system, using a two-step mechanism.

Association data of rFab8 with HEL (which shows apparent nonreversible interaction) (Claudia *et al* 2002) was analysed (figure 10). It fitted into an exponential association, and the Y_{max} obtained was 286 with regression coefficient 0·9994, from the first 6 points (> 70% bind-

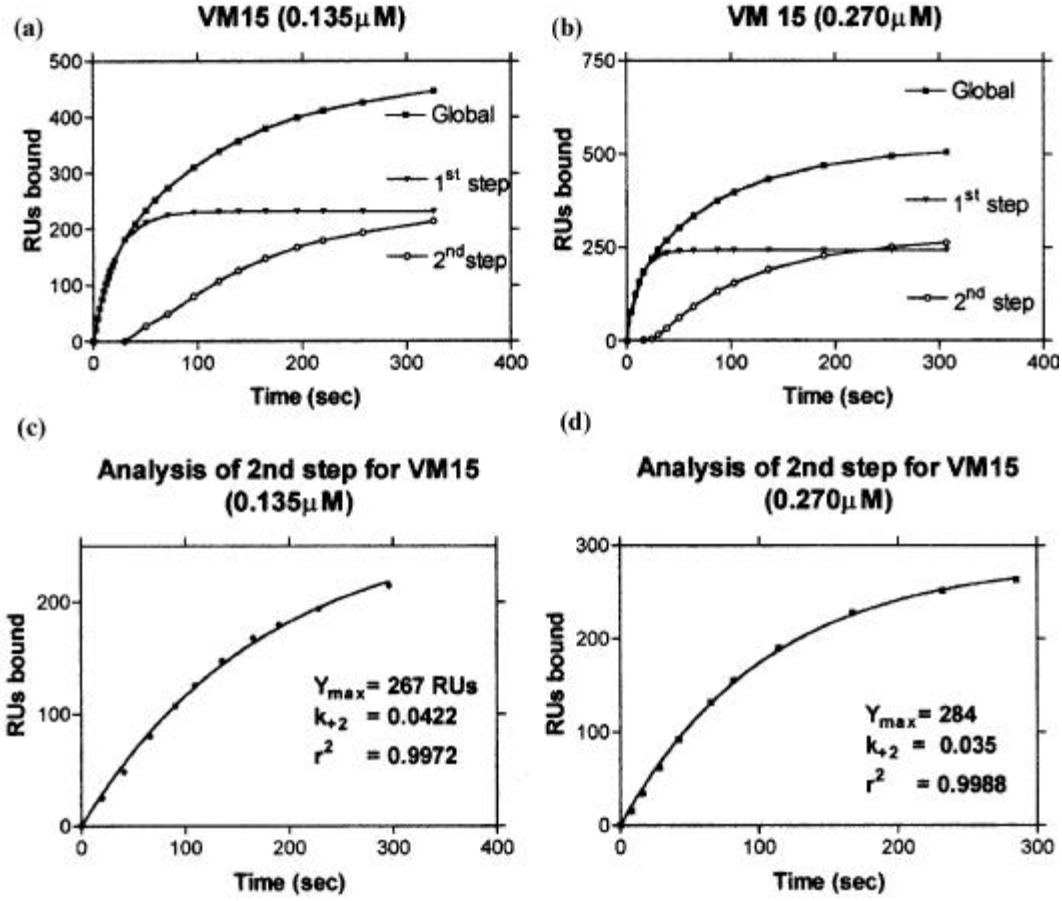

Figure 5. Binding analysis of mAb VM15 at specified concentrations to immobilized hCG (**a** and **b**). (**c** and **d**) Analysis of the second step for the same sensograms. k_{+2} refers to concentration of the analyte multiplied by the second order rate constant of the reaction.

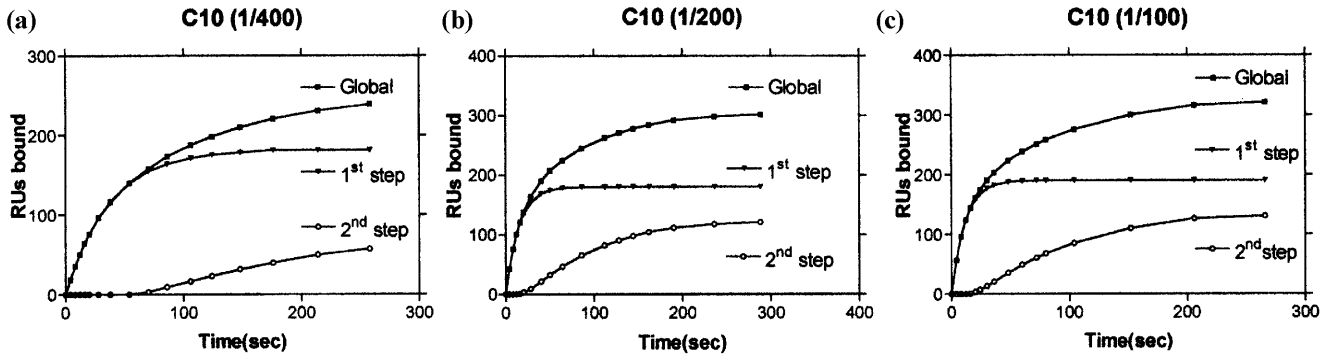

Figure 6. Binding analysis of mAb C10 (culture supernatant) at specified dilutions to immobilized hCG.

Table 1. Kinetic rate constants of mAb-hCG association in BIAcore.

mAb (flow rate)	Conc. (μM)	Y_{max} (RUs)	k_{+1} ($\times 10^{-6}$ M^{-1} s^{-1})	k_{+1}[direct method] ($\times 10^{-6}$ M^{-1} s^{-1}) (figure 7)
VM15 (50 μl/min)	0·135	232	0·362	
	0·270	243	0·333	
	0·540	234	0·304	
VM10 (50 μl/min)	1·080	199	0·028	
	2·160	172	0·034	0·100
	4·320	161	0·031	
VM10 (100 μl/min)	0·864	199	0·033	
VM11 (50 μl/min)	0·054	236	0·113	
	0·108	271	0·103	0·140
	0·216	230	0·143	
VM11 (100 μl/min)	0·108	243	0·120	
	0·216	239	0·134	
	0·432	244	0·163	
C10*	1/400	212	0·027	
	1/200	202	0·028	
	1/100	219	0·022	

*Pseudo first order rate constants normalized to 1/100 dilution.

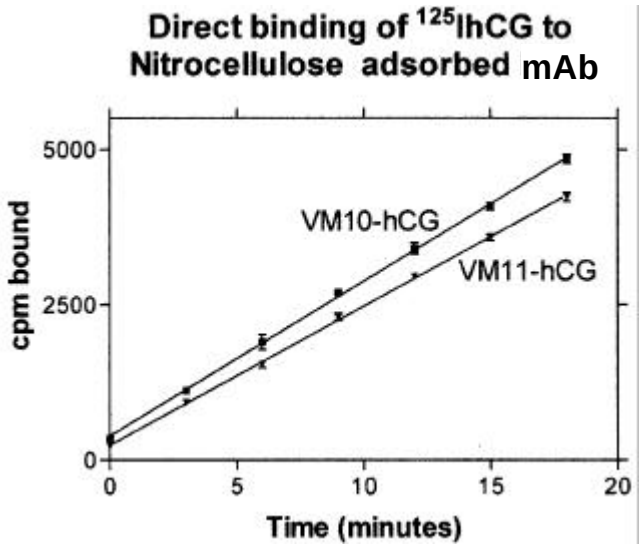

Figure 7. Binding of IhCG to nitrocellulose adsorbed mAb with time. The capacity of the discs were 15 ng/disc (VM10) and 12 ng/disc (VM11). Reaction volume was 2 ml in both cases [IhCG 100,000 (VM10), 85000 (VM11)]. Slopes of association was 249 and 223 cpm/min for VM10 and VM11 respectively. The rate constant was calculated as described under §2.

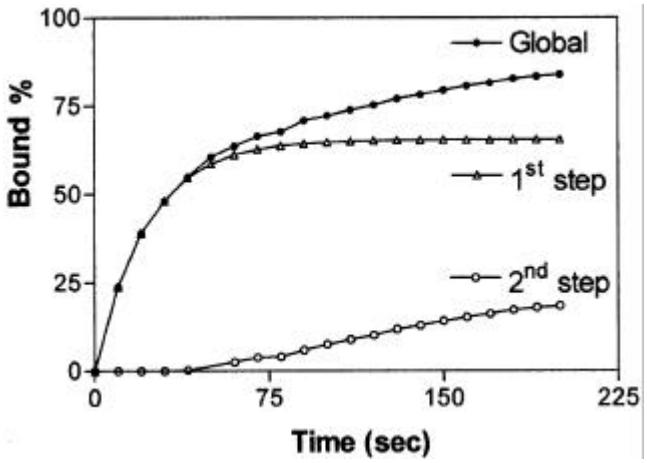

Figure 8. Analysis of the binding of Con-A to CM-dextran (figure 1a from Kalinin *et al* 1995 has been reanalysed).

ing considered). The association beyond 750 s does not fit well, and indicates additional reaction, as shown by us in figure 4b. Another association data by the same authors (sensogram of rFab26 with HEL), showing good dissociation, was analysed using the same approach (figure 11a). The association data fitted into a single exponential (figure 11a). However the dissociation was non-ideal (figure 11b). It may be noted here that one of the essential assumptions in the development of the software analysis in the BIAcore is that the dissociation is ideal. The association followed the classical second order kinetics despite the apparent dissociation demonstrated. This observation is an experimental evidence indicating very little impact of the dissociation in the early part of association in kinetic evaluations.

The heterogeneity of binding observed can be explained kinetically on the basis of a two-step analysis of the sensogram. This analysis indicates that the formation of

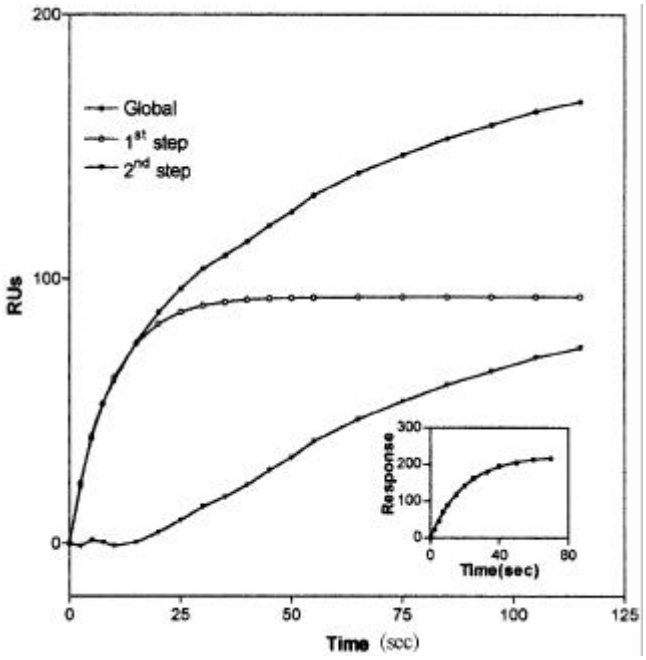

Figure 9. Analysis of the binding of a cyclic peptide to lipid-A (figure 1b from Thomas *et al* 1999 has been reanalysed). Inset shows the reanalysis of the binding of UEA1 to H-antigenic fucolipid (figure 2 from Thomas and Surolia 2000).

the second complex is directly related to the quantity of the first complex formed (demonstrated by the lag phase). A kinetic explanation would be that the first complex binds to the second molecule of the mAb, with a lower association rate. While it is kinetically satisfactory, to this day there has not been a report of an antigen-mAb complex combining with an additional molecule of mAb. An alternative explanation to account for all the kinetic observations is offered, based on the sterical restraints imposed on the mAb to percolate into the interior of the cell during the reaction, in the following discussions.

Chemical coupling of the hCG on the matrix is considered to result in uniform distribution of the hCG in the cell. A cross-section of the flow cell of the BIAcore is represented in figure 12. In our experiments, hCG bound to the cell (60 nl in volume measuring approximately 2000 × 500 × 60 microns) is 6 ng, which corresponds to 1×10^{11} molecules. On binding to the mAb, the combined diameter of the complex becomes 200 Å. Thus, in the first step, the surface hCG reacts and this complex spreads uniformly on the surface of the cell as seen on surfaces 'A' and 'B'. In addition, the presence of inactive (during coupling) hCG, almost equal to that of the reactive hCG, is also spread between these molecules. These two together hinder the flow of the mAb molecules into the interior of

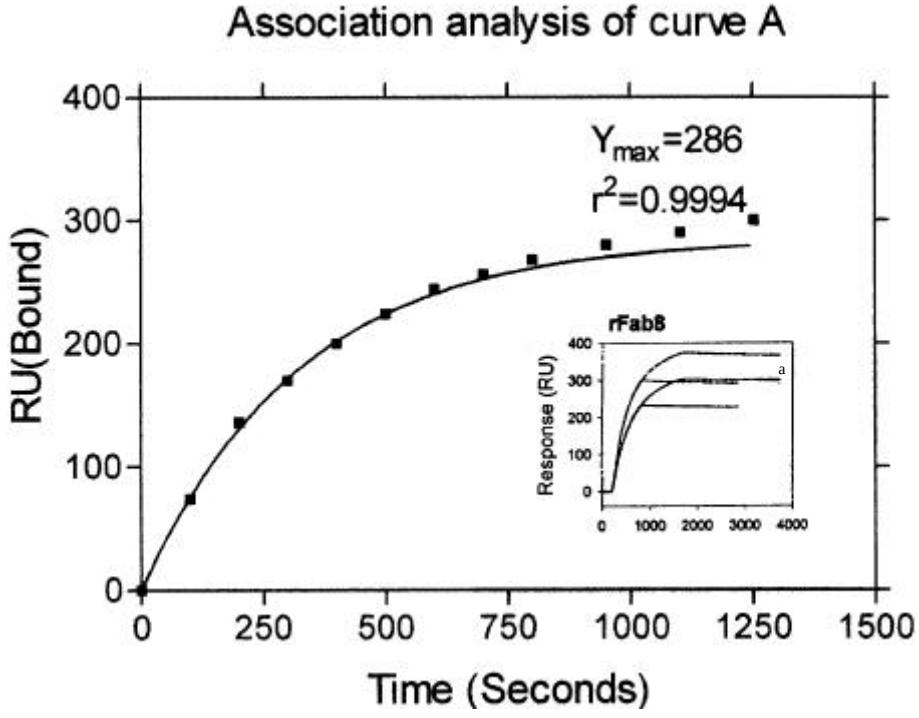

Figure 10. Reanalysis of the data on the association of rFab8 to immobilized HEL (figure 2 from Claudia *et al* 2000). Points in figure are from curve 'a' in the inset. The curve shows the exponential fit taking the first 6 points (covering 70% of the association).

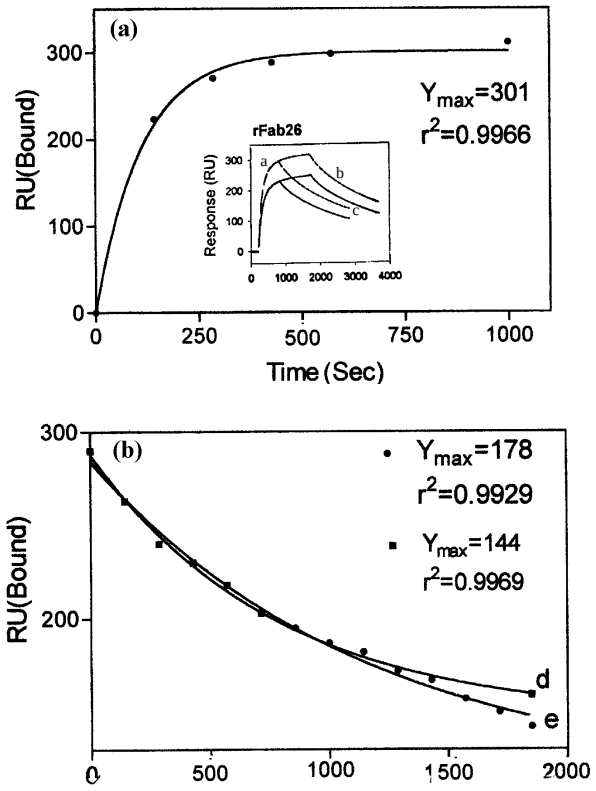

Figure 11. Reanalysis of the association and dissociation sensogram for binding of rFab26 and HEL (figure 2 of Claudia *et al* 2000). The points in **a** are from curve 'a' in the inset. (**b**) The fit of the dissociation for curve 'c' in the inset of '**a**'. Curve 'e' represents the best fit for ideal dissociation using the 12 points, while curve 'd' represents the dissociation projected using the first 6 points (> 50% dissociation).

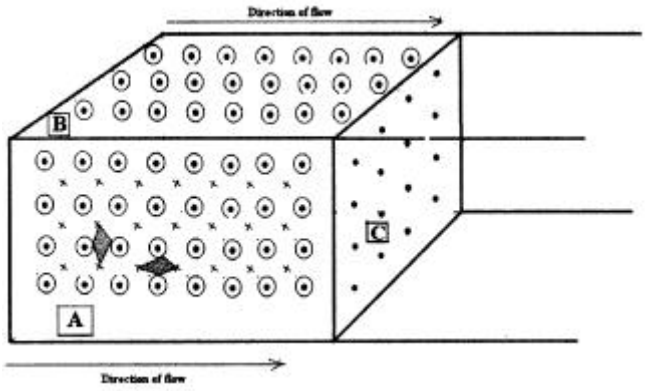

Figure 12. (•) Dots present immobilized hCG (approx. diameter 40 Å).The distance between hCG molecules is calculated to be 800 Å. (⊙) hCG to which mAb is bound. The average diameter of this complex is expected to be 200 Å. (×) hCG which has lost binding property (inactivated) on immobilization. A, B, Surface area of the cell; C, interior of the cell. ( ) Shaded area represents the 'molecular sieve' generated by the binding of mAb to the hCG on the periphery of the cell. (Dimension ~ 600 Å × 800 Å).

the cell, as shown in C. Thus, the second reaction (occurring at the inside of the cell, surface C) is severely restricted by the reaction generated 'molecular sieve'. The quantity of the mAb that can pass through this 'molecular sieve' is determined by the diffusion of the mAb through the pore (grey areas). Thus, at low concentrations of mAb, the second binding is insignificant, and as the concentration of the antibody is increased the diffusion increases resulting in the second interaction (figures 4–6). This would explain qualitatively and quantitatively the lag phase observed and also offers an explanation to the observation that at high mAb concentration Y_{max2} can be greater than Y_{max1} (figure 5d). Diffusion arising exclusively from cross linked dextran fails to explain the presence of [mAb]-dependent lag phase. Thus the only parameters that can be obtained accurately from the sensogram are the Y_{max} and k_{+1}, through the analysis of the early part of the binding curve. The results also suggest that the mechanism of reaction in the BIAcore can best be explained by the following equations.

$$\text{hCG} + \text{mAb} \rightarrow \text{hCG-mAb} \quad (6)$$

$$\text{mAb} \leftrightarrows \text{mAb} + \text{hCG} \rightarrow \text{hCG-mAb}. \quad (7)$$

Equation 6 represents the reaction of the mAb with hCG on the surface of the chip. Eq. 7 represents the diffusion of the mAb into the chip, a rate limiting step for the second reaction. Though both the reactions are chemically identical, the rate limiting nature of the diffusion of the mAb into the interior of the cell explains the anomalous kinetics of the binding reaction.

In conclusion, we have developed a method for analysis of the global fit of the binding of mAb to hCG in BIAcore. The sensogram fits to a two-step model. The second step can be best explained on the basis of formation of a molecular sieve at the surface of the cell, preventing easy diffusion of the mAb into the cell. Longer injection periods can however indicate towards the presence of multiple such low affinity binding sites. The k_{+1} and Y_{max} for the first step is however independent of any uncertainties and can be obtained reproducibly, irrespective of the concentration of the circulated analyte (mAb in this case) as long as the pseudo first order conditions are not violated. It is also suggested that such reaction be carried out at a high flow rate, > 50 µl/min to conform to pseudo-first order conditions. A short sensogram of 2 min duration is adequate for this purpose.

Acknowledgements

The authors thank the Department of Science and Technology, New Delhi for financial support and Prof. Rajan Dighe, for the kind gift of mAb C10 culture supernatant.

References

Banerjee A, Srilatha N S and Murthy G S 2002 Real-time kinetic analysis of hCG-monoclonal antibody interaction using radiolabeled hCG probe: presence of two forms of Ag-mAb complex as revealed by solid phase dissociation studies; *Biochim. Biophys. Acta* **1569** 21–30

Bornhauser S W, Eggenberger J, Jelesarov I, Bernard A, Berge C and Bosshard H R 1998 Thermodynamics and kinetics of the reaction of a single chain antibody fragment (scFv) with the leucine zipper domain of transcription factor GCN4; *Biochemistry* **37** 13011–13020

Chaiken I, Rose S and Karlsson R 1992 Analysis of macromolecular interactions using immobilized ligands; *Anal. Biochem.* **201** 197–210

Claudia A Lipschultz, Yili Li and Sandra Smith-Gill 2000 Experimental Design for analysis of Complex Kinetics Using Surface Plasmon Resonance; *Methods* **20** 310–318

Kalinin N L, Ward L D and Winzor D J 1995 Effects of solute multivalence on the evaluation of binding constants by biosensor technology: studies with concanavalin A and interleukin-6 as partitioning proteins; *Anal. Biochem.* **228** 238–244

Malmqvist M 1993 Biospecific interaction analysis using biosensor technology; *Nature* (*London*) **361** 186–187

McCloskey N, Turner M W and Goldblatt D 1997 Correlation between the avidity of mouse-human chimeric IgG subclass monoclonal antibodies measured by solid phase elution ELISA and biospecific interaction analysis BIA; *J. Immunol. Methods* **205** 67–72

Murthy G S and Moudgal N R 1986 Use of epoxysepharose for protein immobilization; *J. Biosci.* **10** 351–358

Muslin A J, Tanner W J, Allen P M and Shaw A S 1996 Interaction of 14-3-3 with signaling proteins is mediated by the recognition of phosphoserine; *Cell* **84** 889–897

Nieba L, Krebber L and Pluckthun A 1996 Competition BIAcore for measuring true affinities: large differences from values determined from binding kinetics; *Anal. Biochem.* **234** 155–165

Pellequer J L and Van Regenmortel M H V 1993 Measurement of kinetic binding constants of viral antibodies using a new biosensor technology; *J. Immunol. Methods* **166** 133–143

Thomas C J and Surolia A 2000 Kinetic analysis of the binding of Ulex europeas agglutinin 1 (UEA 1) to H-antigenic fucolipid; *Arch. Biochem. Biophys.* **374** 8–12

Thomas C J, Surolia N and Surolia A 1999 Surface plasmon resonance studies resolve the enigmatic endotoxin neutralizing activity of polymyxin B; *J. Biol. Chem.* **274** 29624–29627

Venkatesh N and Murthy G S 1997 Immunochemical approach to the mapping of an assembled epitope of human chrionic gonadotropin: proximity of CTP-*a* to the receptor binding region of the *b*-subunit; *J. Immunol. Methods* **202** 173–182

Venkatesh N, Nagraja G and Murthy G S 1995 Analysis of a conformation specific epitope of the alpha subunit of human chorionic gonadotropin: Study using monoclonal antibody probes; *Curr. Sci.* **69** 48–56

Yamaji A, Sekizawa Y, Emoto K, Sakuraba H and Inoue K 1998 Lysenin a novel sphingomyelin specific binding protein; *J. Biol. Chem.* **273** 5300–5306

MS received 31 March 2003; accepted 18 December 2003

Corresponding editor: SAMIR BHATTACHARYA